Available online at www.sciencedirect.com
SCIENCE DIRECT®
Scripta Materialia 53 (2005) 351–355
Scripta MATERIALIA
www.actamat-journals.com

Effect of anisotropic grain boundary properties on grain boundary plane distributions during grain growth

Jason Gruber [a,*], Denise C. George [b], Andrew P. Kuprat [b], Gregory S. Rohrer [a], Anthony D. Rollett [a]

[a] Department of Materials Science and Engineering, Carnegie Mellon University, 5000 Forbes Avenue, PA 15213, USA
[b] Theoretical Division, Los Alamos National Laboratory, MS B221, Los Alamos, NM 87545, USA

Received 14 December 2004; received in revised form 25 March 2005; accepted 4 April 2005
Available online 13 May 2005

Abstract

The effects of anisotropic grain boundary properties on the evolution of boundary plane distributions were studied using three-dimensional finite element simulations of normal grain growth. The distribution of boundary planes was affected by energy anisotropy whereas no effect was observed for comparatively larger mobility anisotropy.

Keywords: Grain growth; Grain boundaries; Grain boundary energy; Grain boundary mobility; Anisotropy

1. Introduction

The distribution of grain boundary types in a polycrystalline material has been shown to affect its bulk properties, e.g. corrosion resistance [1]. Grain boundary populations are specified by the grain boundary character distribution, $\lambda(\Delta g, n)$, which is the relative areas of distinguishable grain boundaries parameterized by their lattice misorientation (Δg) and boundary plane orientation (n) [2]. Previous experimental work has demonstrated that significant texture can appear in grain boundary character distributions and that low energy boundaries occur in these distributions with greater frequency than higher energy boundaries [2,3].

The influence of anisotropic grain boundary properties on grain growth has been examined previously using two-dimensional grain growth simulations [4–7]. The conclusion from each of these studies was that the grain boundary energy anisotropy was more influential than the mobility anisotropy in determining the distribution of grain boundary types. However, two-dimensional simulations are unable to reproduce the topological complexity of three-dimensional systems or to represent the five-dimensional domain of grain boundary character. A number of papers describe three-dimensional grain growth simulations, but these were calculated under the assumption of isotropic grain boundary properties [8–12]. One of these methods (GRAIN3D) was recently used to simulate growth in a system with anisotropic grain boundary energies and successfully reproduced an experimentally observed grain boundary character distribution [13]. The purpose of the present work is to examine the relative effects of anisotropic interfacial energy and mobility on the grain boundary character distribution in materials undergoing normal grain growth in three dimensions.

2. Simulations

The simulation results are provided by a three-dimensional finite element model using the code GRAIN3D,

* Corresponding author. Tel.: +1 412 268 3044; fax: +1 412 268 3113.
E-mail address: jgruber@andrew.cmu.edu (J. Gruber).

1359-6462/$ - see front matter © 2005 Acta Materialia Inc. Published by Elsevier Ltd. All rights reserved.
doi:10.1016/j.scriptamat.2005.04.004

which is described in detail elsewhere [12,14]. Briefly, GRAIN3D approximates the interfaces in a grain boundary network as a mesh of triangular elements. Nodal velocities are calculated by minimizing a functional that depends on the local geometry of the mesh and the (anisotropic) properties of the grain boundaries. Grain boundary properties are assigned on the basis of the grain boundary character. The interfacial energy $\gamma(\Delta g, \mathrm{n})$ and mobility $M(\Delta g, n)$ functions we use are defined by an interface plane scheme, in which we imagine each boundary to be comprised of the two surfaces bounding the grains on either side of the interface [2]. Taking n^1 to be the interface normal pointing into grain one and indexed in the crystal reference frame of that grain, and n^2 to be the interface normal pointing into grain two and indexed in the crystal reference frame of that grain, the energy and mobility are assigned in the following way:

$$\gamma = (E(n^1) + E(n^2))/2 \tag{1}$$

$$M = (\mu(n^1) + \mu(n^2))/2 \tag{2}$$

where the functions $E(n)$ and $\mu(n)$ are chosen as

$$E = \alpha\left[\sum_{i=1}^{3}(|n_i| - 1/\sqrt{3})^2\right] + 1 \tag{3}$$

$$\mu = \beta\left[\sum_{i=1}^{3}(|n_i| - 1/\sqrt{3})^2\right] + 1 \tag{4}$$

where α and β are positive constants. Minima for either functional then occur with normal vectors of $\langle 1\,1\,1\rangle$ type and maxima with normal vectors of $\langle 1\,0\,0\rangle$ type, as illustrated in Fig. 1. Note that Eqs. (3) and (4) imply cubic crystal symmetry. The choice of cubic symmetry minimizes the number of grain boundaries necessary to produce a statistically significant data set and simplifies the analysis. The form of the energy function is also motivated by experimental observations in Al [15].

The anisotropy of the energy function is controlled by the parameter α. With $\alpha = 0$ the function is isotropic and with $\alpha = 0.2957$, the ratio of the minimum to maximum energy is 1/1.25. Similarly, β controls the mobility anisotropy; when $\beta = 0$ the mobility is isotropic and when $\beta = 13.60$, the ratio of the minimum to maximum mobility is 1/12.5. Simulations were run for four situations: (1) isotropic energy and mobility, (2) isotropic energy and anisotropic mobility, (3) anisotropic energy and isotropic mobility, and (4) anisotropic energy and mobility.

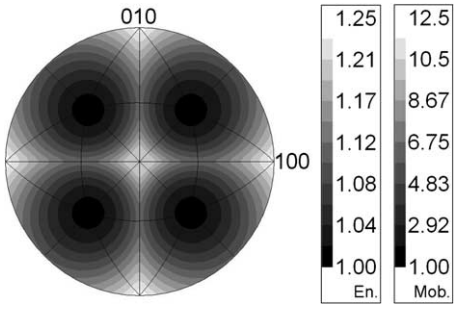

Fig. 1. Energy (En.) and mobility (Mob.) as a function of interface normal vector, [001] stereographic projection. Scale values are in arbitrary units.

The initial microstructure for each simulation was produced from a regular volume-filling tetrahedral mesh of the unit cube. This mesh consisted of 500,000 tetrahedra. Grain centers were assigned randomly to individual tetrahedra with the condition that no grain centers lie in adjacent tetrahedra. After assigning 5000 grain centers, all remaining tetrahedra were assigned to the nearest grain. To produce a relatively equiaxed structure for the simulations, isotropic grain growth was simulated until about half of the grains remained. The mesh that results from this procedure was taken as the starting point for our simulations with anisotropic interfacial properties.

In our simulations, individual grains are represented by collections of tetrahedra, and so any grain boundary is represented by a set of triangular elements. For each triangular element, the lattice misorientation is parameterized by three Euler angles (ϕ_1, Φ, ϕ_2) and the boundary orientation is parameterized by two spherical angles (ϕ, θ). We use discrete binning to measure the relative populations of grain boundaries, with the five-dimensional space of boundary types partitioned into bins of equal volume with sizes of $\Delta\phi_1 = \Delta\phi_2 = \Delta\phi = 10^\circ$ and $\Delta\cos\Phi = \Delta\cos\theta = 1/9$. This discretization results in approximately 6.5×10^3 physically distinct grain boundary types. We assume that making 1.3×10^5 observations, i.e. 20 times the number of distinct boundaries, will produce sufficiently accurate boundary populations. Although each face separating two grains is represented in GRAIN3D as a number of triangular elements, the orientations of the triangles on each face are usually similar. Therefore, as a lower bound, we assume that each face contributes only one distinct orientation. The average grain is bounded by 13–14 faces, each of which is shared with a neighbor grain, and therefore contributes an average of about 6.5–7 observations. It is therefore necessary to have data from more than 20,000 grains to ensure that the total number of observations is at least 20 times the number of distinguishable boundary types. The results from 20 simulations (51,560 grains initially) have therefore been combined to study each case. The results presented here arise from the analysis of data sets with >20,000 grains.

3. Results

The grain boundary plane distributions reached a steady state after a modest amount of growth, as found

previously [13]. This transition period from a nominally uniform distribution to the steady state distribution occurs because of the way we initialized the microstructure. Therefore, only those results characteristic of the steady state behavior are presented. Fig. 2 shows the distributions of grain boundary planes averaged over all misorientations, $\lambda(n)$, after 20,000 grains (~40% of the initial value) have been eliminated. The grain boundary plane distributions for the isotropic case (Fig. 2a) and for the case with anisotropic mobility and isotropic energy (Fig. 2c) are identical and random, i.e. $\lambda(n) = 1.0$ MRD for all n. Whenever the grain boundary energy is anisotropic (Fig. 2b and Fig. 2d) the grain boundary plane distribution is also anisotropic. In the anisotropic distribution, high energy boundary planes occur less frequently than low energy boundary planes. This result is consistent both with experimental observations [2,3] and earlier simulations that did not include mobility anisotropy [13].

The grain boundary plane distributions at two fixed misorientations are shown in Figs. 3 and 4. In each case, these are the distributions after approximately 40% of the grains have been eliminated by growth. The trends observed at these misorientations are similar to those found in the misorientation averaged data (Fig. 2) and at all other fixed misorientations that were examined. When the energy is isotropic, the distribution of grain boundary planes is random, regardless of the mobility. When the grain boundary energy is anisotropic, low energy boundaries have relatively high populations and high energy boundaries occur less frequently. Note that while there is some deviation from the exact random distribution ($\lambda(\Delta g, n) = 1.0$ MRD for all values of Δg and n) with anisotropic mobility and isotropic energy, this deviation is similar to that measured during isotropic growth.

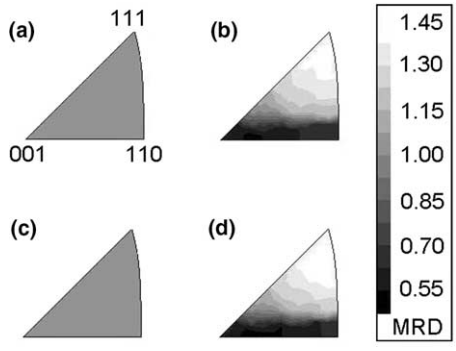

Fig. 2. The distribution of boundary plane types, $\lambda(n)$, independent of misorientation, for (a) isotropic growth; (b) anisotropic energy and isotropic mobility; (c) isotropic energy and anisotropic mobility; and (d) anisotropic energy and mobility. Populations are measured in multiples of random distribution (MRD).

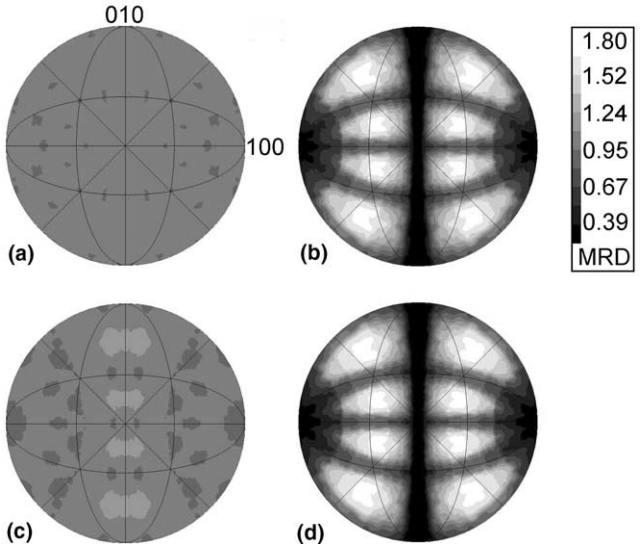

Fig. 3. Grain boundary plane distributions for boundaries misoriented by 45° about [100]: $\lambda(45°/[100], n)$. (a) Isotropic growth; (b) anisotropic energy and isotropic mobility; (c) isotropic energy and anisotropic mobility; and (d) anisotropic energy and mobility. Populations are measured in multiples of random distribution (MRD).

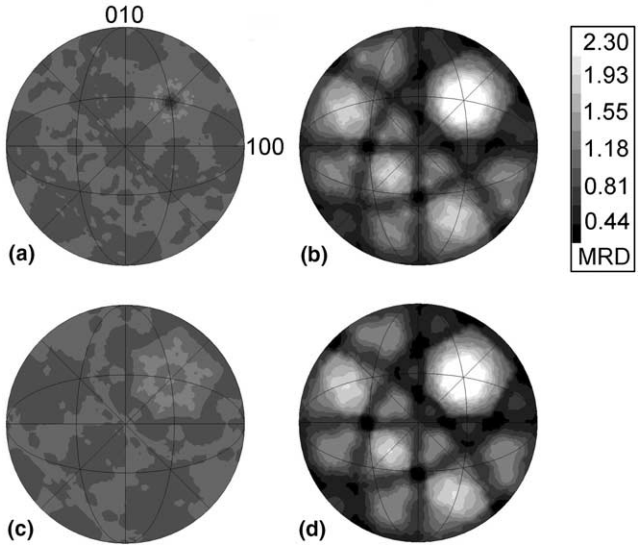

Fig. 4. Grain boundary plane distributions for boundaries misoriented by 60° about [111]: $\lambda(60°/[111], n)$. (a) Isotropic growth; (b) anisotropic energy and isotropic mobility; (c) isotropic energy and anisotropic mobility; and (d) anisotropic energy and mobility. Populations are measured in multiples of random distribution (MRD).

4. Discussion

The results presented here suggest that in polycrystalline materials with random orientation texture, undergoing normal, capillary driven grain growth, the distribution of grain boundary planes is determined by the anisotropy of the energy and is not influenced by the anisotropy of the mobility. This has been

demonstrated by comparing data from selected points in misorientation space (Figs. 3 and 4). To show that this trend persists throughout the entire data set, all grain boundaries were grouped according to their relative energies and relative mobilities. Fig. 5 shows a plot of the mean populations of all boundaries within fixed energy (or mobility) ranges for simulations with anisotropic boundary properties. For each group, we have determined the standard deviation from this average population; this appears in Fig. 5 as bars. There is a clear inverse correlation between the grain boundary energy and population, as noted in an earlier experimental study [2]. By contrast, no effect of anisotropic mobility on grain boundary population was observed.

For the case examined here, the independence of the grain boundary character distribution from the mobility is noteworthy. It should be emphasized that even though the mobility anisotropy was ten times larger than the energy anisotropy, it had a negligible effect on the grain boundary character distribution. In the absence of orientation texture, it might be imagined that the highest mobility boundaries move through grains quickly and are then replaced with random boundary types, reducing the population of high mobility boundaries. However, the results in Fig. 5 demonstrate that this in not the case. In this context it is important to recognize that when the mobility is anisotropic and the energy is isotropic, then the condition for equilibrium at the triple junctions requires that grain boundaries adopt orientations such that the grain boundary dihedral angles are all equal. Therefore, as long as the orientations of the triple lines are randomly distributed, the grain boundary plane orientations will also be randomly distributed, as is the case in Figs. 2a and c. On the other hand, when the boundary energy is anisotropic, the boundaries planes at triple junctions adjust to low energy orientations that also satisfy the interfacial equilibrium constraint and this produces a relatively higher population of low energy boundaries, as suggested in Refs. [5,6]. Finally, it should be noted that we do not necessarily expect the grain boundary character distribution to be independent of mobility when significant orientation texture is present [16].

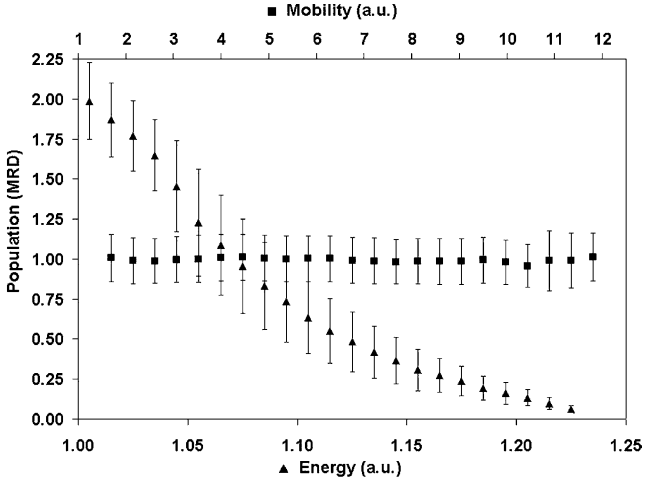

Fig. 5. Average grain boundary plane population for energies within ranges of ±.025 (triangles) and mobilities within ranges of ±0.25 (squares), over the entire domain of energy and mobility values. The energy data are from simulations with anisotropic energy and isotropic mobility. The mobility data are from simulations with anisotropic mobility and isotropic energy. Bars indicate standard deviation from local average.

5. Conclusion

We have studied the relative effects of anisotropic grain boundary energy and mobility on grain boundary character distributions during normal grain growth. The assumed grain boundary energy anisotropy is shown to affect the boundary plane distribution. Boundary plane distributions exhibit relative minima (maxima) for planes at energy maxima (minima), which is consistent with experimental observations and previous simulated results. The assumed grain boundary mobility anisotropy is shown to have no measurable effect on grain boundary plane distributions.

Simulations with anisotropic energy and mobility yielded results that were similar to those obtained with anisotropic energy and isotropic mobility. These results suggest that mobility anisotropy has a relatively small effect on grain boundary plane distributions in comparison to energy anisotropy and with the functions used in this work.

Acknowledgement

This work was supported by the MRSEC program of the National Science Foundation under award number DMR-0079996 and by the Computational Materials Science Network program of the Office of Basic Energy Sciences, Department of Energy.

References

[1] Randle V. Acta Mater 2004;52:4067.
[2] Rohrer GS, Saylor DM, El-Dasher BS, Adams BL, Rollett AD, Wynblatt P. Z Metallknd 2004;95:197.
[3] Saylor DM, Moraweic A, Rohrer GS. Acta Mater 2003;51:3675.
[4] Holm EA, Hassold GN, Miodownik MA. Acta Mater 2001;49:2981.
[5] Upmanyu U, Hassold GN, Kazaryan A, Holm EA, Wang Y, Patton B, et al. Interf Sci 2002;10:201.
[6] Kinderlehrer D, Livshits I, Rohrer GS, Ta'asan S, Yu P. Mater Sci Forum 2004:1063.
[7] Kazaryan A, Wang Y, Dregia SA, Patton BR. Acta Mater 2002;50:2491.

[8] Anderson MP, Grest GS, Srolovitz DJ. Philos Mag B 1989;59:293.
[9] Wegand D, Brechet Y, Lepinoux J, Gust W. Philos Mag B 1999;79:703.
[10] Wakai F, Enomoto N, Ogawa H. Acta Mater 2000;48:1297.
[11] Krill CE, Chen L-Q. Acta Mater 2002;50:3057.
[12] Kuprat AP. SIAM J Sci Comput 2000;22:535.
[13] Gruber J, George DC, Kuprat AP, Rollett AD, Rohrer GS. Mater Sci Forum 2004. p. 733.
[14] Kuprat A, George D, Straub G, Demirel MC. Comput Mater Sci 2003;28:199.
[15] Saylor DM, El Dasher BS, Rollett AD, Rohrer GS. Acta Mater 2004;52:3649.
[16] Rollett AD. JOM 2004;56:63.